Citrinin revisited: from monomers to dimers and beyond

Benjamin R. Clark,[a] Robert J. Capon,*[a] Ernest Lacey,[b] Shaun Tennant[b] and Jennifer H. Gill[b]

Received 20th January 2006, Accepted 27th February 2006
First published as an Advance Article on the web 16th March 2006
DOI: 10.1039/b600960c

Detailed chemical analysis of the solid phase fermentation of an Australian *Penicillium citrinum* isolate has returned the known compounds citrinin (**1**), phenol A acid (**6**), dihydrocitrinone (**7**) and dihydrocitrinin (**8**), together with a novel cytotoxic dimer, dicitrinin A (**5**). Dicitrinin A (**5**) was determined to be a dimerised artefact of the major co-metabolite citrinin, and its structure solved by spectroscopic analysis and chemical modification. Analysis of the products encountered during the controlled decomposition of citrinin led to the discovery of additional citrinin dimers and delineated a plausible mechanistic pathway linking all monomeric and dimeric citrinin degradation products.

Introduction

Well known for the production of biologically active metabolites, *Penicillium citrinum* Thom is a common filamentous fungus found the world over. One of the best known *P. citrinum* metabolites is citrinin (**1**), a polyketide mycotoxin first isolated from a *P. citrinum* strain in 1931.[1] The structure for citrinin (**1**) was first proposed by Brown *et al.* in 1948,[2] although subsequent studies were needed to clarify the absolute stereochemistry[3] and tautomeric configuration.[4] Extensive biosynthetic studies have been carried out on **1** using a variety of isotopic labelling strategies.[5,6] A large number of citrinin derivatives have been isolated, most notably by Curtis *et al.*, who in 1968 described the isolation of seven metabolites related to citrinin.[7]

Citrinin (**1**) is a well-known contaminant of a number of agricultural products, and has been demonstrated to possess nephrotoxic activity[8] in addition to a number of other chronic toxic effects.[9] As such, several studies have been carried out on its detoxification *via* degradation. These studies concluded that decomposition of citrinin occurs at >175 °C under dry conditions, and at lower temperatures (>100 °C) in the presence of water.[10,11] Known citrinin decomposition products include phenol A (**2**) and the formylated derivative citrinin H2 (**3**).[12] In most cases, decomposition of citrinin coincides with a decrease in cytotoxicity, however, at least one study[13] noted that the decomposition of citrinin under aqueous conditions led to an *increase* in cytotoxicity. This increased cytotoxicity was attributed to formation of citrinin H1 (**4**).[13]

The current report provides an account of a chemical investigation into an Australian *P. citrinum* isolate. In addition to describing the isolation and structure elucidation of citrinin and a selection of known analogues, this report presents the first account of a new cytotoxic citrinin dimer, dicitrinin A (**5**). Recognizing that **5** could be an artefact brought about during handling and storage, this study includes a detailed chemical analysis of the decomposition of citrinin under various conditions. This study defines the conditions that led to the sequential transformation of citrinin into both monomeric and dimeric products, and also includes a detailed mechanistic analysis of the decomposition.

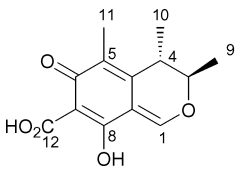

citrinin **(1)**

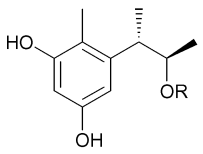

phenol A **(2)** R = H
citrinin H2 **(3)** R = CHO

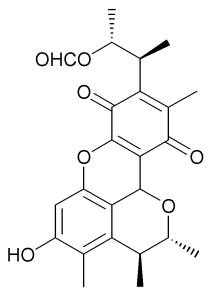

citrinin H1 **(4)**

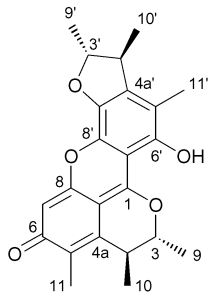

dicitrinin A **(5)**

Results and discussion

The MeOH extract derived from a solid fermentation of *P. citrinum* (MST-F10130) was concentrated *in vacuo* and the residue fractionated by repeated reverse phase SPE and HPLC to yield the known *P. citrinum* metabolites citrinin (**1**), phenol A acid (**6**), dihydrocitrinone (**7**), and dihydrocitrinin (**8**), in addition to the unprecedented citrinin dimer, dicitrinin A (**5**). The known compounds **1**, **6**, **7** and **8** were identified by spectroscopic analysis (HRESIMS, ^{1}H and ^{13}C NMR, UV-vis, and $[\alpha]_{D}$) and comparison to literature data.[8,14–19]

Dicitrinin A (**5**) was isolated as a deep red solid that returned a HRESI(+)MS pseudomolecular ion (M + Na, *m/z* 403.1520) corresponding to a molecular formula ($C_{23}H_{24}O_5$) requiring 12 double bond equivalents (DBE). Examination of the ^{1}H NMR spectrum revealed two isolated spin systems, designated fragments A and B.

[a]*Centre for Molecular Biodiversity, Institute for Molecular Bioscience, University of Queensland, Brisbane, QLD, 4072, Australia. E-mail: r.capon@imb.uq.edu.au; Fax: +61 7 3346 2090; Tel: +61 7 3346 2979*
[b]*Microbial Screening Technologies Pty. Ltd., Smithfield, NSW, 2164, Australia. E-mail: elacey@microbialscreening.com; Fax: +61 2 9757 4515; Tel: +61 2 9757 2586*

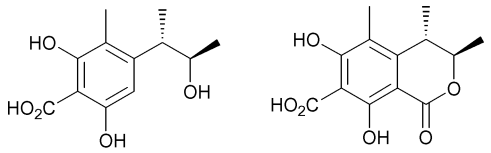

phenol A acid **(6)**

dihydrocitrinone **(7)**

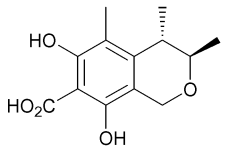

dihydrocitrinin **(8)**

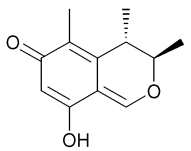

decarboxycitrinin **(9)**

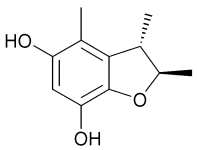

10

The ^{1}H NMR resonances associated with fragment A consisted of two 2° methyls (δ_H 1.26 and 1.37), one deshielded methyl (δ_H 2.22), two methines (δ_H 3.55 and 5.46), and a deshielded singlet (δ_H 7.03). A suite of gCOSY correlations confirmed that the 2° methyls and methines were mutually coupled, and this, together with gHMBC correlations, established the partial structure as indicated (see Fig. 1). All ^{13}C NMR chemical shifts for fragment A were consistent with the assigned structure, with C-1, C-6 and C-8 all deemed sp^2 and oxygenated based on their deshielded chemical shifts (δ_C 169.8, 170.4 and 157.6, respectively). The chemical shifts for C-1 and C-6 in particular, were consistent with the quinone methide indicated. The relative stereochemistry of the 2° methyls in fragment A were determined to be *trans* based on $^{3}J_{3,4}$ (<0.5 Hz) which was comparable to $^{3}J_{3,4}$ values observed for citrinin (**1**). In this regard, fragment A resembles a C-7 decarboxylated "citrinin" akin to decarboxycitrinin (**9**).

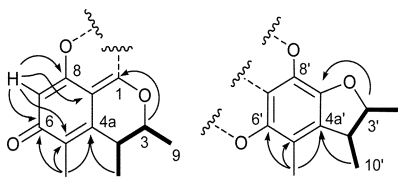

Fig. 1 Structure fragments for dicitrinin A (**5**). Arrows indicate key gHMBC correlations, while bold bonds highlight gCOSY correlations.

The ^{1}H NMR resonances associated with fragment B were similar to those of fragment A, consisting of two 2° methyls (δ_H 1.30 and 1.36), a singlet methyl (δ_H 2.27), and two methines (δ_H 3.42 and 4.75). Again, gCOSY and gHMBC analysis (see Fig. 1) established a partial structure which was strongly reminiscent of the known citrinin analogue **10**.[20] Carbon resonances for C-7′ and C-8′ (δ_C 104.7 and 137.3, respectively) in fragment B, which could not be assigned by gHMBC analysis, were assigned by comparison with literature data for **10** (δ_C 102.8 and 138.9, respectively). The relative configuration about the two 2° methyls in fragment B was assigned by consideration of $^{3}J_{3',4'}$. Although a useful model compound of known *trans* relative stereochemistry, the ^{1}H NMR resonances reported for H-3 and H-4 in **10** were described as multiplets, with no experimental measure of $^{3}J_{3',4'}$.[20] In the absence of experimental data we simulated ^{1}H NMR spectra for **10** with both natural *trans* and unnatural *cis* stereochemistries, returning calculated $^{3}J_{3,4}$ values of 4.0 and 8.2 Hz, respectively. The former value was very close to the experimentally observed $^{3}J_{3',4'}$ value for fragment B (3.6 Hz), suggestive of a *trans*-stereochemistry about these methyls. In this respect fragment B can be viewed as a decarboxylated ring B contracted "citrinin" analogue.

Fragments A and B account for all ^{1}H and ^{13}C NMR resonances observed in the NMR spectra of **5**, however, consideration of the molecular formula confirmed that one DBE and one proton remained unaccounted for, and the two fragments shared a "common" oxygen atom. The missing DBE could be accounted for by requiring that a single ring be formed in the fusion of fragments A and B. Likewise, the "common" oxygen atom could explained if the C-8 oxygen of fragment A was common with one of either the C-6′ or the C-8′ oxygens evident in fragment B. Finally, the missing proton could be attributed to a phenolic proton on fragment B.

Given the partial structures attributed to fragments A and B, and the observations listed above, there existed two alternative ways to assemble the two fragments. The chemical shift for C-7′ (δ_C 104.7) dictated that it could not be oxygenated, thus C-7′ in fragment B must be linked to C-1 in fragment A. Given that the C-8 oxygen in fragment A must be common with either the C-6′ or the C-8′ oxygen in fragment B, the two alternate structures for dicitrinin A are shown in Fig. 2. At this point the available evidence was incapable of unambiguously determining which of these two structures was correct. Efforts at observing an NOE correlation between the phenolic OH and the C-5′ methyl could not be pursued as, despite the use of several alternative NMR solvents, the phenolic OH resonance was not observed in any ^{1}H NMR data set. As an alternative, *O*-methylation of the phenolic OH in **5** was attempted, in an effort to obtain a methyl ether that would reveal the crucial NOE correlations.

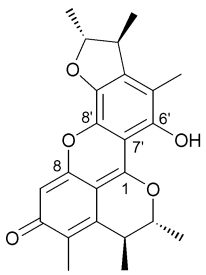

"common" C-8 and C-8′ oxygen (correct)

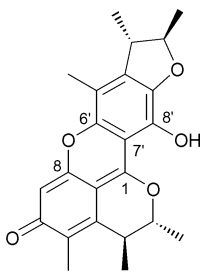

"common" C-8 and C-6′ oxygen (incorrect)

Fig. 2 Plausible alternative structures for dicitrinin A (**5**).

Small scale (*ca.* 100 μg) trial methylations of dicitrinin A (**5**) with MeI proved promising, with LC-DAD-MS analysis confirming the formation of a monomethylated product (*m*/*z* 395, M + H). However, when the methylation was repeated on a larger scale (1.6 mg) the major product (1.1 mg, 64%) proved to be an unexpected dimethylated species **11** (*m*/*z* 409, M). The most noticeable change in the ^{1}H NMR spectrum of dimethyl dicitrinin

Table 1 NMR data (600 MHz, d_6-DMSO) for dicitrinin A (**5**) and dimethyl dicitrinin A (**11**)

Position	Dicitrinin A (**5**)				Dimethyl dicitrinin A (**11**)		
H #	δ_C[a]	δ_H (m, *J*/Hz)	gCOSY	gHMBC	δ_C[b]	δ_H (m, *J*/Hz)	gHMBC
1	169.8				170.8		
3	84.9	5.46 (q, 6.8)	H-9	C-1, C-4, C-4a, C-9, C-10	85.5	5.59 (q, 6.6)	C-1, C-4a
4	33.3	3.55 (q, 7.2)	H-10	C-4a, C-5, C-8a, C-10	33.0	3.65 (q, 7.2)	C-4a, C-5, C-8a, C-9
4a	137.5				136.7		
5	124.1				124.5		
6	170.4				169.4		
7	99.4	7.03 (s)	H-11	C-5, C-6, C-8, C-8a	97.3	7.60 (s)	C-5, C-6, C-8, C-8a
8	157.6				158.0		
8a	102.4				104.2		
9	18.2	1.37 (d, 6.8)	H-3	C-3, C-4	18.3	1.39 (d, 6.6)	C-3, C-4
10	18.8	1.26 (d, 7.2)	H-4	C-3, C-4, C-4a	17.8	1.28 (d, 7.2)	C-3, C-4, C-4a
11	10.0	2.22 (s)	H-7	C-4a, C-5, C-6	10.0	2.27 (s)	C-4a, C-5, C-6
3′	87.9	4.75 (dq, 3.6, 6.4)	H-4′, H-9′	C-4a′, C-8′/8a′, C-10′	88.9	4.85 (dq, 4.0, 6.5)	
4′	44.2	3.42 (dq, 3.6, 7.0)	H-3′, H-10′	C-4a′, C-8′/8a′, C-9′, C-10′	44.2	3.49 (obs)	
4a′	144.9				143.3		
5′	119.1				126.6		
6′	149.3				149.9		
7′	104.7				—		
8′	137.3				—		
8a′	137.2				—		
9′	20.6	1.36 (d, 6.4)	H-3′	C-3′, C-4′	20.3	1.40 (d, 6.5)	C-3′, C-4′
10′	18.7	1.30 (d, 7.0)	H-10′	C-3′, C-4′, C-4a′	18.3	1.34 (d, 7.0)	C-3′, C-4′, C-4a′
11′	12.0	2.27 (s)		C-4a′, C-5′, C-6′	11.3	2.38 (s)	C-4a′, C-5′, C-6′
6-Me					58.8	4.14 (s)	C-6
6′-Me					62.2	3.84 (s)	C-6′

[a] Assignments were assisted by HSQC, HMBC, and DEPT experiments, and by comparison with related compounds. [b] Most ^{13}C values have been extracted from HMBC and HSQC spectra and assigned by comparison to **5**. C-7′, C-8′ and C-8a′ were not observed.

A (**11**), relative to dicitrinin A (**5**), was the appearance of two new methyl singlets (δ_H 4.14 and 3.84, see Table 1) consistent with the presence of two OMe groups. gHMBC correlations from these new OMe groups to carbons at 169.4 and 149.9 ppm, respectively, implied that both the C-6 and C-6′ oxygens had been methylated. While dicitrinin A (**5**) exhibited strong pseudomolecular ions in ESI(+)MS and ESI(−)MS, dimethyl dicitrinin A (**11**) only ionised in the positive mode, returning an exceptionally clean ESI(+)MS spectrum. Even when HRESI(+)MS data was acquired in the presence of a NaI reference, no (M + Na) ion was observed, suggesting that **11** possessed an inherent positive charge. That **11** was cationic was further supported by its high water solubility (compared to **5**, which is EtOAc soluble and water insoluble), and its immobility on silica TLC (*cf.* rf **11** = 0.0 *vs.* **5** = 0.25, with an eluant of 99 : 1 EtOAc–HCO_2H). This cationic character was also apparent from UV-vis studies, described below. This unexpected dimethylation not withstanding, a ROESY NMR experiment carried out on **11** revealed informative correlations between the C-6′ OMe and C-5′ methyl, and between the C-6 OMe and H-7 (see Fig. 1), confirming the relative stereostructures of both dimethyl dicitrinin A (**11**) and dicitrinin A (**5**). The formation and stability of the dimethyl oxonium **11** can be attributed to extensive charge delocalisation as proposed in Fig. 3.

Given the assigned structure for dicitrinin A (**5**) it seemed highly likely that **5** was an artefact brought about by dimerization of the abundant co-metabolite citrinin (**1**). As such, given that the absolute stereochemistry of citrinin is known[3] and the same as citrinin encountered in this study (*i.e.* same $[\alpha]_D$), by inference the absolute stereochemistry of dicitrinin A (**5**) and its dimethyl analogue **11** can be assigned as shown.

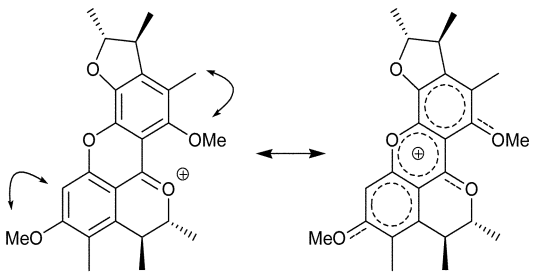

dimethyl dicitrinin A (**11**)

Fig. 3 Dimethyl dicitrinin A (**11**). Arrows indicate key ROESY correlations. Extended resonance delocalization stabilizes the oxonium.

UV-vis studies

The UV-vis spectrum of **5** was observed to undergo reversible pH sensitive shifts (see Fig. 4). Under basic conditions a dramatic shift was observed in the λ_{max} of the electron-transfer band at 422 to 540 nm. Such bathychromic shifts are well known for deprotonated phenolic compounds,[21] although the magnitude of the shift was unusually high in this case. Under acidic conditions another change in the UV-vis spectrum occurred, with the appearance of a new peak at 490 nm, attributed to the formation of a protonated species. Curiously, all dicitrinins occur as red solids, but are bright yellow in solution. This colour change may be indicative of an amphoteric character, with the solid form being composed partially or fully of a "salt" comprised of oxonium and oxyanion species such as those given in Fig. 4. Consistent with this hypothesis, dimethyl dicitrinin A (**11**), which is no longer amphoteric, forms a yellow solid.

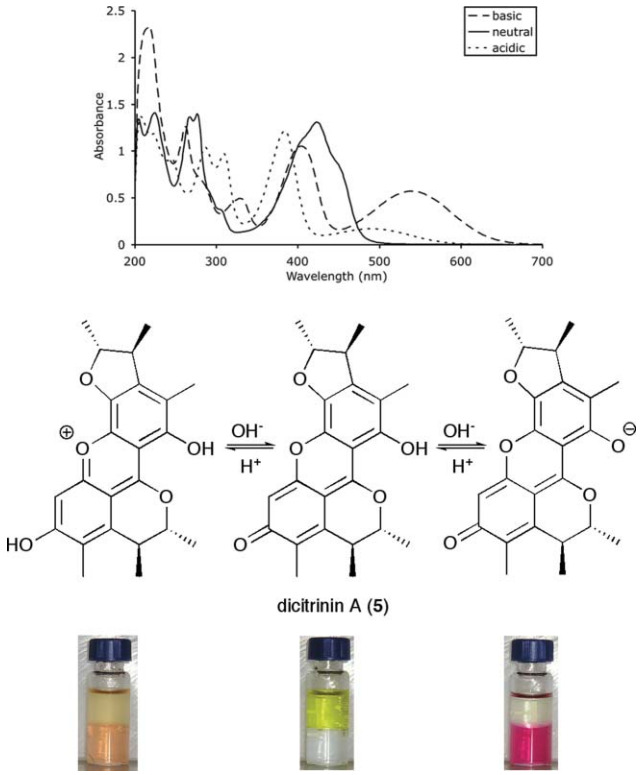

Fig. 4 UV-vis spectra of dicitrinin A (**5**) under different pH conditions, and speculated products. Vial images are EtOAc–H_2O partitions.

The dimethyl derivative **11** also displayed interesting changes in its UV-vis spectrum (see Fig. 5). Not surprisingly, addition of acid resulted in no change, however, under basic conditions the prominent peaks at 449 and 379 nm disappeared entirely. It was speculated that the dramatic change in the UV-vis spectrum was due to nucleophilic addition of OH^- at C-1, which quenched the oxonium moiety and disrupted the extended conjugation (see Fig. 5). Further evidence for a nucleophilic addition adduct was obtained by LC-DAD-MS analysis of a sample of **11** to which NaOH had been added, which revealed a single peak (*m*/*z* 449, M + Na) consistent with the proposed product shown in Fig. 5. This change in the UV-vis spectrum of **11** proved to be reversible, although attempts to effect comparable changes with nucleophiles other than hydroxide proved unsuccessful.

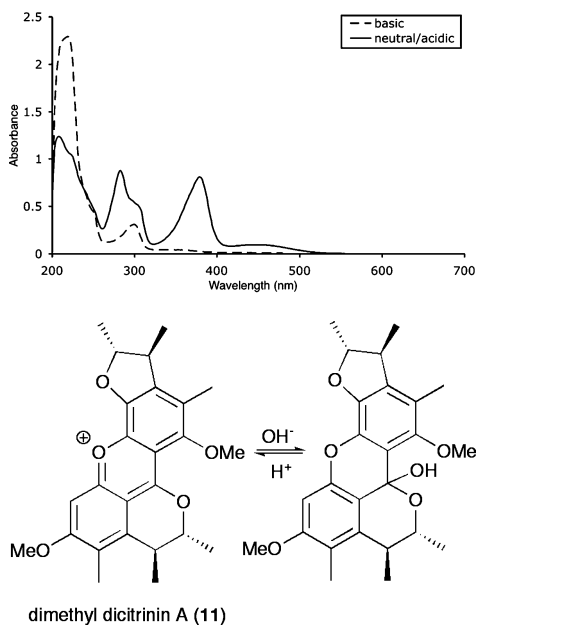

Fig. 5 UV-vis spectra of dimethyl dicitrinin A (**11**) under different pH conditions, and speculated products.

Decomposition studies

After elucidation of the structure of dicitrinin A (**5**), consideration was given to the hypothesis that **5** was an artefact of the handling and/or storage procedures. Initial decomposition studies were designed to mimic the conditions encountered during fractionation: *i.e.*, mild heating, and exposure to mild acid and base.

Two samples of citrinin (10 mg each) were dissolved in aqueous MeOH (4 mL), with one sample being acidified with a drop of trifluoroacetic acid (TFA), and the other basified with a drop of triethylamine (TEA). The two samples were heated at 50 °C in sealed flasks for 7 d and their decomposition progress monitored by LC-DAD-MS. The presence of TEA appeared to stabilise the citrinin (**1**) and no significant decomposition was observed. However, under TFA conditions decomposition did occur, yielding products that were *tentatively* identified as phenol A (**2**), phenol A acid (**6**) and decarboxycitrinin (**9**) based on LC-DAD-MS analysis. No dimeric products were observed. This result prompted a second set of decompositions at higher concentration, in the hope of promoting dimerization. For solubility reasons these studies were carried out in MeOH. Three samples of citrinin (**1**) (5 mg each) were dissolved in a small amount of MeOH (100 μL), with a drop of TFA added to one, TEA to another; and the third left unmodified. All three samples were heated at 50 °C in sealed vials over a period of 15 d, with the reaction progress monitored by LC-DAD-MS. Under neutral conditions dicitrinin A (**5**) was formed as a major product. Dicitrinin A (**5**) was also formed in both the TFA and TEA modified samples, however yields were not as high, with TEA slowing the decomposition and TFA favouring the formation of monomeric products.

To further investigate the identities of the decomposition products, the experiment was repeated on a larger scale (50 mg), under neutral conditions in MeOH (0.5 mL). The reaction was halted after 14 d and LC-DAD-MS analysis of the crude decomposition mixture performed (see Fig. 6).

The resulting mixture was then fractionated by reverse phase HPLC: details of the major products are presented in Table 2. The major product was dicitrinin A (**5**), with an estimated yield of *ca.* 8 mg (16%). Other known compounds isolated from the mixture included all of the monomeric species detected in the earlier aqueous methanol decompositions. Three new dimeric products (**12**–**14**) were isolated and their identities are addressed below.

A noteworthy feature of the decomposition products was their different behaviour during ESIMS analysis. While all products formed strong M + H ions under ESI(+)MS conditions, two different ionisation processes were observed during ESI(−)MS acquisition-leading to either M − H or M + 17 ions as the dominant species. It is known that citrinin exists as a hydrate (**15**) in aqueous solution (see Fig. 10),[14] so it is reasonable to assume that decomposition products bearing an analagous quinone methide

Table 2 Data for major compounds isolated from large-scale citrinin (**1**) decomposition

Compound	Yield/mg	Major ions (+ve)	Major ions (−ve)	UV-vis maxima[a]
Phenol A (**2**)	3.3 (6.6%)	197 (M + H)	195 (M − H), 179 (M − 17)	282, 223 (sh), 202
Phenol A acid (**6**)	4.2 (8.4%)	241 (M + H)	239 (M − H)	315, 252, 214
Decarboxycitrinin (**9**)	1.5 (3.0%)	207 (M + H)	223 (M + H_2O − H), 205 (M − H)	336, 288, 228 (sh), 203
Dicitrinin D (**14**)	0.9 (1.8%)	437 (M + H)	453 (M + H_2O − H)	413 (sh), 394, 267, 232
Citrinin (**1**)	1.0 (2.0%)	251 (M + H)	267 (M + H_2O − H)	409 (sh), 332, 236
Dicitrinin C (**13**)	<0.7 (1.4%)	393 (M + H)	409 (M + H_2O − H)	450 (sh), 425 (sh), 378, 293 (sh), 269, 230
Dicitrinin A (**5**)	8.0 (16%)	381 (M + H)	379 (M − H)	516 (sh), 451 (sh), 422 (sh), 385, 308, 279, 223[b]
Dicitrinin B (**12**)	<0.8 (1.6%)	383 (M + H)	381 (M − H)	408, 281, 267, 241

[a] Extracted from DAD. [b] This UV-vis spectrum does not correspond to any of those shown in Fig. 2, due to the presence of protonated species.

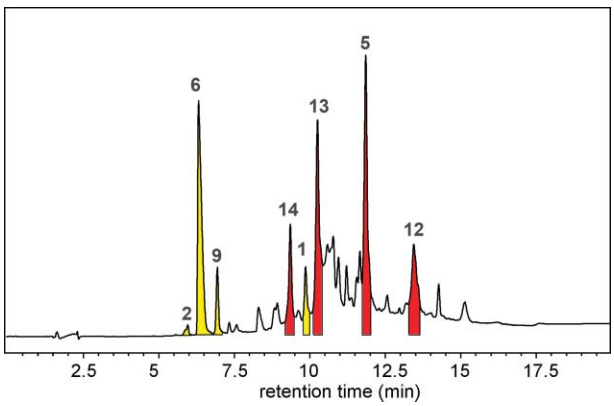

Fig. 6 HPLC DAD trace (254 nm) from the decomposition of citrinin (**1**). Details for major peaks are given in Table 2. Yellow peaks represent monomeric species while red peaks correspond to dimeric species.

moiety could generate hydrated ions (*i.e.* M + H_2O–H) under ESI(−)MS conditions. Those products that bear a phenolic OH might be expected to suppress this ion forming pathway, in favor of the more direct formation of an M − H ion. Consistent with this hypothesis, decarboxycitrinin (**9**) exhibits both M − H and M + H_2O − H ions in the ESI(−)MS, whereas phenols **2** and **6**, which lack the capacity to form hydrates show only M − H ions. In the ESI(−)MS of dicitrinin A (**5**) the M − H ion dominates as hydration at C-1 would disrupt the extended conjugation. This "hydrated ion" hypothesis proved a valuable tool in exploring possible structures for the new citrinin dimers, dicitrinins B–D (**12**–**14**).

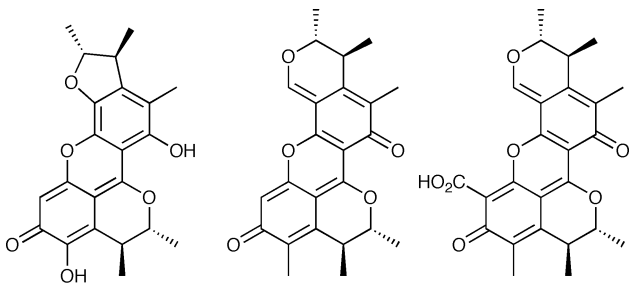

Of the new dicitrinins only dicitrinin B (**12**) returned useful ^{1}H NMR data. The ^{1}H NMR spectrum of **12** was very similar to that of **5**, consisting of four 2° methyls (δ_H 1.21, 1.27, 1.28 and 1.32), an aromatic methyl (δ_H 2.34), four methines (δ_H 3.24, 3.29, 4.57 and 5.01), a deshielded singlet (δ_H 6.29), and a broad exchangeable resonance (δ_H 9.81). The molecular formula of **12** ($C_{22}H_{22}O_6$) established by HRESI(+)MS analysis (*m*/*z* 383.1495, M + H), was consistent with the oxidative cleavage of an aromatic methyl in dicitrinin A (**5**). ^{1}H NMR chemical shifts and 2D NMR correlations for **12** were consistent with this assessment, and gHMBC correlations confirmed placement of the aromatic methyl at C-5′, implying that the C-5 methyl had been cleaved. gHMBC correlations from H-3, H-4 and H_3-10 to a common carbon (δ_C 110.6), assigned as C-4a, supported this hypothesis. The ^{13}C NMR resonance for C-4a (δ_C 110.6) in **12** was significantly shielded relative to C-4a in **5** (δ_C 137.5), as would be predicted by the placement of a hydroxy group at C-5. The arguments presented above permit a *tentative* structure assignment to dicitrinin B (**12**) as indicated. The ESI(−)MS spectra of **12** was dominated by an M − H ion, as predicted. A plausible mechanism for the oxidative transformation of dicitrinin A (**5**) into dicitrinin B (**12**) is presented in Fig. 7.

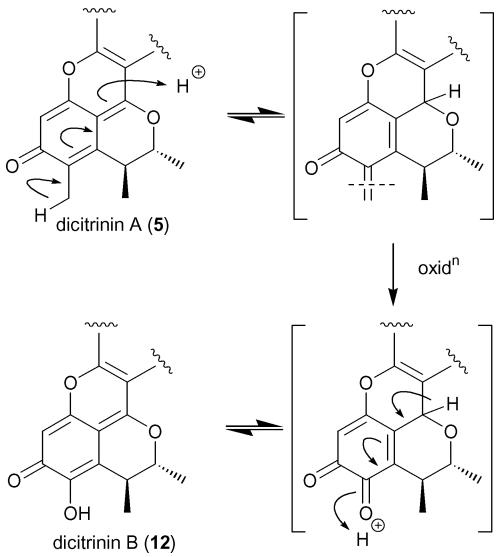

Fig. 7 Proposed mechanism for the oxidative conversion of dicitrinin A (**5**) to yield dicitrinin B (**12**).

In the absence of NMR data the structures *tentatively* proposed for dicitrinins C (**13**) and D (**14**) rely heavily on mass spectral and UV-vis analysis, and consideration of likely decomposition outcomes. HRESI(+)MS analysis revealed molecular formulae for **13** ($C_{24}H_{24}O_5$) and **14** ($C_{25}H_{24}O_7$) suggestive that the former was a dicitrinin A analogue that had not undergone ring contraction, whereas the latter was a dicitrinin C precursor that had not undergone decarboxylation. While by necessity *speculative*,

the proposed structures are consistent with the available data, and represent plausible intermediates along the decomposition pathway from citrinin to dicitrinins A and B. The ESI(−)MS for dicitrinin C (**13**) and D (**14**) are dominated, as predicted, by M + H_2O − H ions. Plausible mechanisms for a ring contraction of dicitrinin C (**13**) to yield dicitrinin A (**5**), and a decarboxylation of dicitrinin D (**14**) to yield dicitrinin C (**13**), are shown in Fig. 8 and 9, respectively.

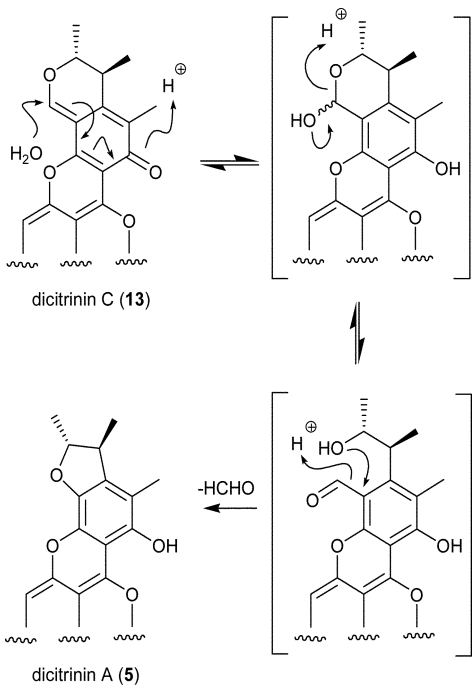

Fig. 8 Proposed mechanism for the ring contraction conversion of dicitrinin C (**13**) to yield dicitrinin A (**5**).

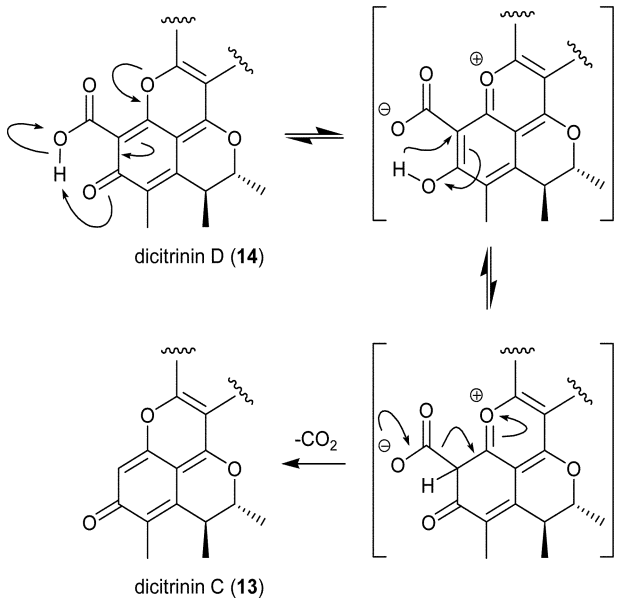

Fig. 9 Proposed mechanism for the decarboxylation of dicitrinin D (**14**) yield dicitrinin C (**13**).

The mechanisms proposed in Fig. 7–9, that address decomposition processes of oxidation, ring contraction and decarboxylation, respectively, delineate key stages in the interconversion of dicitrinins. These processes, together with the formation of citrinin hydrate, keto/enol tautomerization, redox and hydroysis can also be used to explain the formation of monomeric citrinin decomposition products. A plausible citrinin decomposition pathway linking all monomeric species mentioned in this report is shown in Fig. 10. A key driver for the proposed pathway is the ability of citrinin (**1**) to form the hydrate **15**. A redox reaction between **1** and **15** can lead to the oxidized product dihydrocitrinone (**7**) and the reduced product dihydrocitrinin (**8**). Likewise, **15** can ring open to lead to **2**, **3** and **6**, or ring open and then ring contract to give **10**.

Having proposed the majority of the decomposition pathway, the key "dimerization" event remains to be explained. A plausible mechanism for dimerization of citrinin (**1**) is presented in Fig. 11. This mechanism involves a heterocyclic Diels–Alder connection between citrinin (**1**) and an alternate citrinin tautomer, followed by the irreversible loss of CO_2 and H_2O to form a key intermediate. This hypothetical intermediate, which was not detected in our studies, may undergo oxidation to re-establish the quinone methide and extended conjugation, leading to dicitrinins A–D. Alternatively this intermediate can undergo oxidative ring opening to give citrinin H1 (**4**).

While the structures for dicitrinins B–D (**12–14**) are only *tentatively* assigned, the discussion presented on dicitrinin A (**5**), including spectroscopic and mechanistic observations, reveals citrinin as an entry point into hitherto underexplored chemical space. It is interesting to speculate on the range of Diels–Alder products that could be obtained by challenging citrinin by an array of natural and synthetic dienophiles. Curiously, nature has provided a glimpse into such space with the timely report by Kobayashi *et al.* in 2005[22] of perinadine A (**16**) from a marine-derived strain of *P. citrinum* Perinadine A (**16**) represents a natural mixed citrinin and pyrrolidine alkaloid Diels–Alder adduct.

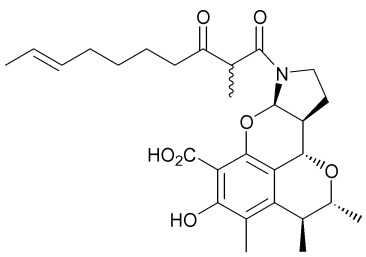

In the current study, all purified compounds were screened against a range of test microorganisms, and against the mouse NS-1 cell line. None possessed significant antimicrobial activity, but citrinin (**1**) and dicitrinin A (**5**) were moderately active in the NS-1 cytotoxicity assay, with LD_{99} values of 25 and 6.3 μg mL^{-1}, respectively.

Our experimental protocols and mechanistic hypotheses, detailed above, for the conversion of citrinin (**1**) into both monomeric and dimeric decomposition products provides a comprehensive molecular basis for future analytical chemistry investigations into citrinin-contaminated foods and their detoxification. To support these studies we are also seeking to investigate the formation

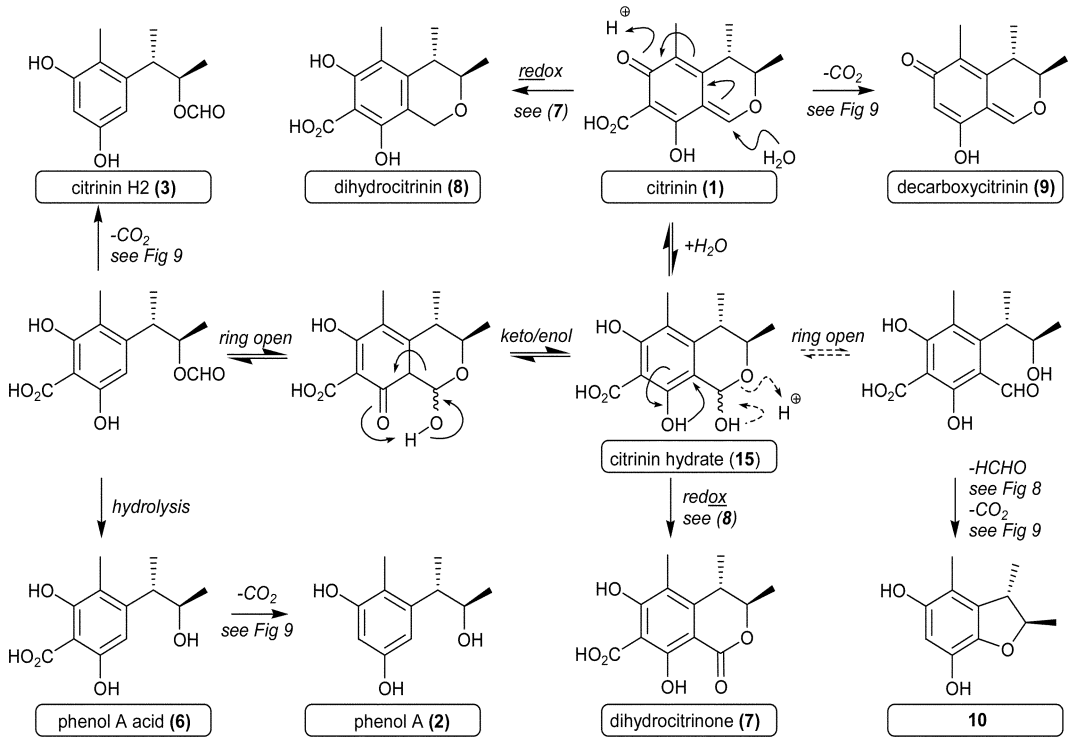

Fig. 10 Proposed mechanism for the decomposition of citrinin (**1**) into monomeric species.

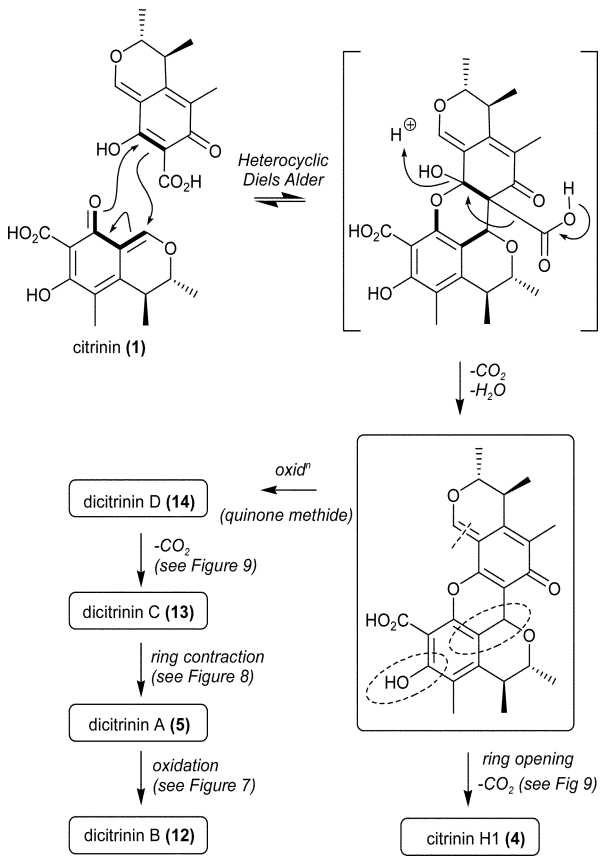

Fig. 11 Proposed mechanism for the dimerization of citrinin (**1**), and subsequent formation of dicitrinins A–D and citrinin H1.

of Diels–Alder adducts between citrinin and a range of natural and synthetic dienophiles. The results from these studies will be reported at a future date.

Experimental

General experimental procedures have been described previously.[23] NMR spectrum simulations were carried out using ACD HNMR Predictor software, version 7.

Analytical HPLC gradients

Standard LC-DAD-MS analyses were carried out using the following gradient: 1 mL min^{-1} gradient elution from 90% H_2O–MeCN (0.05% HCO_2H) to MeCN (0.05% HCO_2H) using a 5 μm Zorbax StableBond C_8 150 × 4.6 mm column.

Assays

Details for antimicrobial and cytotoxicity assays have been described.[24]

Biological material

The fungal strain (MST-F10130) was isolated from a roadside soil sample collected near Ardlethan in New South Wales, Australia. The isolate was identified as *Penicillium citrinum* Thom on morphological grounds.

Isolation

A solid fermentation (1 kg wheat, 21 d, 28 °C) was extracted twice with MeOH (*ca.* 6 L). These extracts were combined and

concentrated *in vacuo* to an aqueous concentrate (2 L) and triethylamine added to adjust to pH *ca.* 8.5. This was passed through four parallel C_{18} SPE cartridges (4 × 10 g, Varian HF C_{18}) followed by sequential elution with 50% H_2O–MeOH (4 × 40 mL each) and MeOH (4 × 40 mL each). The aqueous eluant was adjusted to pH *ca.* 3.5 with the addition of trifluoroacetic acid (TFA) and once more passed through the same C_{18} SPE cartridges followed by similar sequential elution to afford 50% H_2O–MeOH and MeOH fractions. All 50% H_2O–MeOH and MeOH eluants were evaporated to give a combined residue (*ca.* 7.9 g). This was subjected to preparative HPLC (60 mL min^{-1} with gradient elution of 70 to 40% H_2O–MeCN (0.01% TFA) over 20 min followed by MeCN (0.01% TFA) for 10 min, through a 5 mm Phenomenex Luna $C_{18(2)}$ 50 × 100 mm column), giving 10 fractions.

One of the combined fractions was partitioned between butanol and water, and the butanol-soluble material subjected to preparative HPLC (22 mL min^{-1} gradient elution from 70 to 30% H_2O–MeCN over 16 min, through a 5 μm Zorbax RX–C_8 21.2 × 250 mm column) to yield citrinin (**1**) (130 mg) and dihydrocitrinin (**8**) (9 mg). Another of the combined fractions was also partitioned between butanol and water, and the water-soluble material further purified by HPLC (2.5 mL min^{-1} gradient elution from 85 to 33% H_2O–MeCN, through a 5 μm Zorbax StableBond C_{18} 9.4 × 250 mm column) to give phenol A acid **6** (6 mg).

One of the more polar fractions was re-subjected to preparative HPLC (60 mL min^{-1} with isocratic elution of 79% H_2O–MeCN (0.01% TFA) over 30 min, through a 5 μm Phenomenex Luna $C_{18(2)}$ 50 × 100 mm column), followed by C_{18} SPE (Alltech C_{18} Extract-clean 2 g cartridge, 10% stepwise gradient elution from 80 to 100% MeOH) to give dihydrocitrinone (**7**) (18 mg) and dicitrinin A (**5**) (8 mg).

Citrinin (1). Identified by spectroscopic analysis. $[\alpha]_D$, ESI(±)MS, ^{1}H and ^{13}C NMR were in good agreement with literature values.[8,14]

Dicitrinin A (5). Red solid; $[\alpha]_D$ +73.9° (*c* 0.016, $CHCl_3$); IR $\nu_{max}(CHCl_3)/cm^{-1}$ 3495, 2985, 2932, 1618, 1533, 1455, 1411, 1381; UV-vis λ_{max}(EtOH)/nm 446 (sh) ($\varepsilon/dm^3mol^{-1}cm^{-1}$ 7300), 422 (10500), 401 (sh) (8900), 304 (3400), 293 (sh) (4500), 276 (11100), 267 (11000), 223 (12100); UV-vis λ_{max}(EtOH–HCl)/nm 490 ($\varepsilon/dm^3mol^{-1}cm^{-1}$1300), 384 (9500), 309 (7600), 286 (8200), 245 (7200), 223 (9100), 208 (10400); UV-vis λ_{max}(EtOH–NaOH)/nm 540 ($\varepsilon/dm^3mol^{-1}cm^{-1}$ 4600), 403 (8400), 329 (4000), 283 (sh) (5400), 262 (10100), 218 (br) (18600); ^{1}H NMR (d_6-DMSO, 600 MHz) see Table 1; ^{13}C NMR (d_6-DMSO, 150 MHz) see Table 1; ESI(+)MS *m/z* 381 (M + H); ESI (−) MS *m/z* 379 (M–H); HRESI(+)MS *m/z* 403.1520 (M + Na, $C_{23}H_{24}O_5Na$ requires 403.1521).

Phenol A acid (6). Identified by spectroscopic analysis. $[\alpha]_D$, ESI(±)MS, ^{1}H NMR and ^{13}C NMR were in good agreement with literature values.[16–18]

Dihydrocitrinone (7). Identified by spectroscopic analysis. $[\alpha]_D$, ESI(±)MS, ^{1}H and ^{13}C NMR were in good agreement with literature values.[15,25]

Dihydrocitrinin (8). Identified by spectroscopic analysis. $[\alpha]_D$, ESI(±)MS, ^{1}H and ^{13}C NMR were in good agreement with literature values.[19]

Dimethyl dicitrinin A (11). Dicitrinin A (**5**) (1.6 mg) was dissolved in dry EtOAc (0.5 mL) after which Na_2CO_3 (10 mg) and an excess of MeI (50 μL) were added, and the mixture stirred overnight at 50 °C. The mixture was then filtered and evaporated to dryness. Purification of the product was carried out using C_8 HPLC (3.2 mL min^{-1} gradient elution from 60 to 30% H_2O–MeCN (0.1% TFA) over 20 min, through a 5 μm Zorbax C_8 10 × 250 mm column), to give dimethyl dicitrinin A (**11**) as a yellow solid (1.1 mg, 64%). UV-vis λ_{max}(EtOH)/nm 449 ($\varepsilon/dm^3mol^{-1}cm^{-1}$ 830), 379 (6800), 306 (sh) (4100), 282 (7400), 208 (10400); UV-vis λ_{max}(EtOH–NaOH)/nm 299 ($\varepsilon/dm^3mol^{-1}cm^{-1}$ 2600), 251 (sh) (4600), 219 (19200); ^{1}H NMR (d_6-DMSO, 600 MHz) see Table 1; ^{13}C NMR (d_6-DMSO, 150 MHz) see Table 1; ESI(+)MS *m/z* 409 (M); HRESI(+)MS *m/z* 409.2012 (M, $C_{25}H_{29}O_5$ requires 409.2015).

Decomposition Studies

For the small scale "dilute" solution decompositions, the following procedure was used. Two duplicate samples of citrinin (**1**) (10 mg) were dissolved in aqueous MeOH (1 : 1, 4 mL) in vials, and a drop of TFA added to one and TEA to the other. The vials were then sealed and the mixture stirred at 50 °C for 4 d. Reaction progress was monitored by LC-DAD-MS.

The small scale "concentrated" solution decompositions were carried out in sealed vials. Three duplicate samples of citrinin (**1**) (5 mg) were each dissolved in MeOH (100 μL) in vials. A drop of TFA was added to one vial, a drop of TEA to another, and no additive to the third. The sealed mixtures were heated at 50 °C for 15 d, and reaction progress monitored by LC-DAD-MS.

The large-scale decomposition was carried out in the same manner, using 50 mg (0.2 mmol) of **1** in 0.5 mL MeOH, for 15 d. Fractionation of the products formed in the large-scale decomposition was carried out using C_{18} HPLC (22 mL min^{-1} gradient elution from 20% H_2O–MeCN (0.1% TFA) to MeCN (0.1% TFA) over 30 min, through a 5 μm Zorbax StableBond-C_{18} 21.2 × 250 mm column) to yield phenol A (**2**) (3.3 mg, 6.6%), phenol A acid (**6**) (4.2 mg, 8.4%), and dicitrinin A (**5**) (8.0 mg, 16%) as the major products. A small quantity of unreacted citrinin (**1**) (1.0 mg, 2%) was also recovered, while decarboxycitrinin (**9**) (estimated 1.5 mg) was isolated but decomposed before analysis. Three minor dimers, dicitrinin B (**12**) (0.8 mg, 1.6%), dicitrinin C (**13**) (0.7 mg, 1.4%) and dicitrinin D (**14**) (0.9 mg, 1.8%) were also isolated. UV-vis spectra for dicitrinins B–D were extracted from DAD data-reported extinction coefficients are relative only.

Phenol A (2). Identified by spectroscopic analysis. ESI(±)MS, ^{1}H NMR and ^{13}C NMR were in good agreement with literature values.[17,18]

Dicitrinin B (12). A red solid; UV-vis λ_{max}(MeCN–H_2O)/nm 408 ($\varepsilon/dm^3mol^{-1}cm^{-1}$ 9200), 281 (7300), 267 (6500), 241 (10000); δ_H(600 MHz, d_6-DMSO) 9.81 (brs, OH), 6.29 (s, H-7), 5.01 (q, *J* 5.9, H-3), 4.57 (dq, *J* 6.4, 4.2, H-3′), 3.29 (obs, H-4′), 3.24 (q, *J* 6.8, H-4), 2.34 (s, H_3-11), 1.32 (d, *J* 6.4, H_3-9′), 1.28 (d, *J* 6.9, H_3-10′), 1.27 (d, *J* 5.9, H_3-9), 1.21 (d, *J* 6.8, H_3-10); ESI(+)MS *m/z* 787 (2M + Na), 383 (M + H); ESI(−)MS *m/z* 381 (M–H); HRESI(+)MS *m/z* 383.1495 (M + H, $C_{22}H_{23}O_6$ requires 383.1495).

Dicitrinin C (13). A red solid; UV-vis λ_{max}(MeCN–H_2O)/nm 450 (sh) (ε/dm^{3}mol^{-1}cm^{-1} 2300), 425 (sh) (3200), 378 (7800), 293 (sh) (2900), 269 (10000), 230 (6600); ESI(+)MS m/z 393 (M + H); ESI(−)MS m/z 841 (2M + Na + 2H_2O − 2H), 409 (M + H_2O − H); HRESI(+)MS m/z 393.1703 (M + H, $C_{24}H_{25}O_5$ requires 393.1702).

Dicitrinin D (14). A red solid; UV-vis λ_{max}(MeCN–H_2O)/nm 413 (sh) (ε/dm^{3}mol^{-1}cm^{-1} 8000), 394 (8800), 267 (10000), 232 (7100); ESI(+)MS m/z 895 (2M + Na), 437 (M + H); ESI(−)MS m/z 453 (M + H_2O − H); HRESI(+)MS m/z 437.1598 (M + H, $C_{25}H_{25}O_7$ requires 437.1600).

Acknowledgements

The authors would like to acknowledge A. Hocking for taxonomic studies and G. MacFarlane for acquisition of HRMS data. B. Clark was the recipient of a SGSA scholarship from the University of Queensland. This research was partially funded by the Australian Research Council.

References

1 A. C. Hetherington and H. Raistrick, *Philos. Trans. R. Soc. London, Ser. B*, 1931, **220**, 269–296.
2 J. P. Brown, N. J. Cartwright, A. Robertson and W. B. Whalley, *Nature*, 1948, **162**, 72–73.
3 R. K. Hill and L. A. Gardella, *J. Org. Chem.*, 1964, **29**, 766–767.
4 S. Kovac, P. Nemec, V. Betina and J. Balan, *Nature*, 1961, **190**, 1104–1105.
5 L. Colombo, C. Gennari, D. Potenza, C. Scolastico, F. Aragozzini and C. Merendi, *J. Chem. Soc., Perkin Trans. 1*, 1981, 2594–2597.
6 J. Barber, A. C. Chapman and T. D. Howard, *J. Antibiot.*, 1987, **40**, 245–248.
7 R. F. Curtis, C. H. Hassall and M. Nazar, *J. Chem. Soc. C*, 1968, 85–93.
8 P. Krogh, E. Hasselager and P. Friis, *Acta Pathol. Microbiol. Scand., Sect. B: Microbiol. Immunol.*, 1970, **78**, 401–413.
9 V. Betina, *Mycotoxins: Chemical, Biological, and Environmental Aspects*, Elsevier, Amsterdam, 1989.
10 N. Kitabatake, A. B. Trivedi and E. Doi, *J. Agric. Food Chem.*, 1991, **39**, 2240–2244.
11 A. B. Trivedi, E. Doi and N. Kitabatake, *J. Food Sci.*, 1993, **58**, 229–232.
12 M. Hirota, A. B. Menta, K. Yoneyama and N. Kitabatake, *Biosci., Biotechnol., Biochem.*, 2002, **66**, 206–210.
13 A. B. Trivedi, M. Hirota, D. Etsushiro and N. Kitabatake, *J. Chem. Soc., Perkin Trans. 1*, 1993, 2167–2171.
14 J. Barber, J. L. Cornford, T. D. Howard and D. Sharples, *J. Chem. Soc., Perkin Trans. 1*, 1987, 2743–2744.
15 M. M. Chien, P. L. Schiff, Jr., D. J. Slatkin and J. E. Knapp, *Lloydia*, 1977, **40**, 301–302.
16 N. J. Cartwright, A. Robertson and W. B. Whalley, *J. Chem. Soc.*, 1949, 1563–1567.
17 T. Roedel and H. Gerlach, *Liebigs Ann.*, 1995, 885–888.
18 J. P. Brown, A. Robertson, W. B. Whalley and N. J. Cartwright, *J. Chem. Soc.*, 1949, 867–879.
19 J. Deruiter, J. M. Jacyno, R. A. Davis and H. G. Cutler, *J. Enzyme Inhib.*, 1992, **6**, 201–210.
20 C.-H. Chen, C.-Y. Shaw, C.-C. Chen and Y.-C. Tsai, *J. Nat. Prod.*, 2002, **65**, 740–741.
21 A. I. Scott, *Interpretation of the Ultraviolet Spectra of Natural Products*, Pergamon Press, Oxford, 1964.
22 M. Sasaki, M. Tsuda, M. Sekiguchi, Y. Mikami and J. Kobayashi, *Org. Lett.*, 2005, **7**, 4261–4264.
23 B. R. Clark, R. J. Capon, E. Lacey, S. Tennant and J. H. Gill, *Org. Biomol. Chem.*, 2006, DOI: 10.1039/b600959j.
24 B. Clark, R. J. Capon, M. Stewart, E. Lacey, S. Tennant and J. H. Gill, *J. Nat. Prod.*, 2004, **67**, 1729–1731.
25 C. H. Hassall and D. W. Jones, *J. Chem. Soc.*, 1962, 4189–4191.

